Optical investigation of tunneling in AlAs/GaAs/AlAs double-barrier diodes

S. R. Andrews*
GEC-Marconi, Ltd., Hirst Research Centre, East Lane, Wembley, Middlesex HA9 7PP, United Kingdom

A. J. Turberfield
Department of Physics, University of Oxford, Clarendon Laboratory, Parks Road, Oxford OX1 3PU, United Kingdom

B. A. Miller†
GEC-Marconi, Ltd., Hirst Research Centre, East Lane, Wembley, Middlesex HA9 7PP, United Kingdom
(Received 5 November 1992)

We describe time-integrated and time-resolved photoluminescence measurements made on a series of *n*-type symmetric and asymmetric AlAs/GaAs/AlAs double-barrier tunneling diodes. Optical measurements of the electron charge buildup in the well near the peak in the tunneling current are used to deduce the average dwell time. This is found to be shorter than expected for tunneling through a Γ-point AlAs collector barrier for barriers thicker than about 3 nm but can be explained if there is strong scattering into *X*-point valleys. Under high-intensity illumination we also observe a substantial photoexcited hole current with clear tunneling peaks together with accumulation near the collector barrier and in the well.

I. INTRODUCTION

Tunneling through double-barrier semiconductor structures has been the subject of many studies in recent years because of interest in the fundamentals of tunneling and also because of possible applications to *mm*-wave transistors, local oscillators, detectors, mixers, and multistate logic devices. Double-barrier tunneling diodes (DBTD's) generally consist of doped contact layers between which lie two wider band-gap undoped barrier layers and an intervening quantum well. Such structures can exhibit regions of strong negative differential conductivity (NDC). Two models of tunneling are commonly used in interpreting the behavior of such devices. In the coherent model, the phase coherence of the carrier wave function is preserved in the tunneling process and a resonant enhancement of the transmitted probability can occur under conditions of constructive interference of the multiply reflected waves, analogous to that at the transmission peak of a Fabry-Perot interferometer. Such resonant tunneling can take place when the energy of a quasibound state in the quantum well coincides with that of occupied states in the emitter possessing the same in-plane wave vector,[1] a condition which can be achieved by the application of a bias. We will use the term resonant sparingly, however, since the observation of NDC does not require coherent transport through the structure and can be understood qualitatively even if the coherence of the electron wave function is destroyed by inelastic scattering in the well. In fact, this might be expected since the electron dwell time in the well, sometimes called the transit time, is typically long compared with acoustic- or optic-phonon emission rates.[2,3] In the incoherent case described by the so-called sequential tunneling model,[4,5] NDC is a consequence of tunneling through the emitter barrier into quasi-two-dimensional states in the well with a loss of phase information, with the result that tunneling through the collector barrier takes place independently. In real devices, the width of the injected carrier distribution is much greater than the width of the resonance in the coherent model, and the observable quantities such as current and dwell time are insensitive to weak inelastic scattering which merely broadens the resonance.[3] This has made it difficult to resolve experimentally the question of whether the transport preserves any coherent character in practice.[3,6] However, in the strong-scattering case, the predictions of the two models are the same only if the transmission of the collector barrier is much greater than that of the emitter barrier. Under bias this is always true for symmetric diodes, which have identical emitter and collector barriers, but not necessarily for asymmetric diodes which have a collector barrier much thicker than the emitter barrier. It is then possible for the current density to be much larger and the resonant-state lifetime much shorter in the incoherent case than in the coherent case because of scattering into states for which the collector barrier is more transparent. More generally, similar behavior is predicted for any DBTD in which there are strong irreversible scattering processes in the well, such as intersubband relaxation.[7]

Optical measurements can in principle offer insights into majority-carrier charge accumulation and decay in the quantum well during tunneling;[3,8–18] they also enable us to study transport and accumulation of optically excited minority carriers in the same device. In most optical studies of transport in DBTD's, the barrier layers were made of the direct-gap alloy $Al_xGa_{1-x}As$ ($x < 0.45$) separated and bounded by the direct-gap material GaAs. Here, we report time-integrated and time-resolved photoluminescence (PL) measurements of (electrically injected) electron and (optically injected) hole transport and charge accumulation in symmetric and asymmetric

AlAs/GaAs/AlAs diodes which have indirect band-gap barriers. It is generally assumed that the magnitude of the resonant-tunneling current in such structures is determined by the conduction-band barrier height at the Γ point in the Brillouin zone, and that inelastic scattering into X-point extrema, where the barrier is lower, contributes only to the valley current.[19–21] We show below that this is a special case and that it is possible for the peak tunneling current and transit time in asymmetric devices to be strongly modified by the inelastic-scattering rate between Γ-point GaAs electron states in the quantum-well and zone-boundary states associated with the transverse X valleys ([010] and [001]) in the AlAs collector barrier. A preliminary report of some of the experiments can be found in Ref. 22.

The paper is organized as follows. In Sec. II, details of the structures and experimental methods are presented. In Sec. III, a model for the radiative recombination mechanism and PL and PL excitation (PLE) data is presented. Optical measurements of the electron density in the well and a discussion of electron transport through the collector barrier are presented in Sec. IV, followed by a summary in Sec. V.

II. EXPERIMENTAL DETAILS

Four structures were designed to allow a systematic study of the relationship between the optical and transport properties of the DBTD's. The generic structure consists of Si-doped n-type and undoped (ud) layers grown by molecular-beam epitaxy at 580 °C in the following order on n^+-type [100] GaAs substrates: 0.4-μm GaAs (n-2×10^{18} cm^{-3}); ten periods 4.2-nm GaAs/3.1-nm AlAs (n-2×10^{18} cm^{-3}); 85-nm GaAs (n-N_D); 4.2-nm GaAs spacer (ud), AlAs barrier (ud) thickness L_{b1}; 5.1-nm GaAs quantum well (ud), AlAs barrier (ud) thickness L_{b2}; 4.2-nm GaAs spacer (ud); 85-nm GaAs (n-N_D); and 85-nm GaAs (n-2×10^{18} cm^{-3}). The thicknesses of the last two layers were chosen so that in most of the optical experiments approximately equal fractions of the exciting light entering the structure would be absorbed on either side of the double barrier. The undoped spacer layers reduce dopant diffusion into the barriers. The superlattice buffer was incorporated in an attempt to improve the growth of subsequent layers and has no significant effect on the transport or optical properties described below. Layer thicknesses were determined to within two monolayers by transmission-electron microscopy measurements. Barrier thicknesses L_{b1} and L_{b2} are given in Table I. Diodes S have symmetric tunneling barriers ($L_{b1}=L_{b2}$) and diodes A are asymmetric. N_D was determined by electrochemical profiling to be in the range 2–3×10^{17} cm^{-3} for diodes $S1$, $S2$, and $A1$ and ~5×10^{17} cm^{-3} for $A2$. Using values for N_D in this range, we obtained good agreement between the measured and calculated biases for the peak tunneling current in the dark (solving Poisson's equation in the Boltzmann approximation and neglecting quantization in the emitter).

TABLE I. Diode parameters: barrier widths and typical peak tunneling currents and corresponding dark voltages in forward (f) and reverse (r) bias.

Diode	L_{b1}	L_{b2}	I_p^f (meas.)	I_p^r (meas.)	V_p^f	V_p^r
$S1$	2.5 nm	2.5 nm	15 mA	14 mA	0.70	−0.65
$A1$	2.5 nm	5.1 nm	11 mA	~1 μA	1.10	−0.50
$A2$	3.5 nm	5.1 nm	0.92 mA	15 μA	0.41	−0.31
$S2$	5.1 nm	5.1 nm	3.6 μA	3.3 μA	0.32	−0.28

Mesa geometry devices with areas of 10^{-4} cm^2 were prepared using standard optical lithography and wet etching techniques. Shallow Ni-Ge-Au Ohmic contacts were formed to mesa top and bottom (both on the same side of the wafer to minimize series resistance) with a 50-μm-square aperture in the top contact for optical access.

Continuous-wave (cw) PL and PLE measurements were performed using an argon-ion pumped pyridine two-dye laser as the excitation source. Time-resolved spectra were excited with a synchronously pumped dye laser and detected using a single grating monochromator and streak camera with a system resolution of order 25 ps.

Figure 1 shows schematically the band lineups in a biased device. The devices show clear NDC in their current-voltage (I-V) characteristics at 5 K, where all the measurements and calculations described in this paper were performed. Table I gives details of four-terminal measurements of the current and bias at the tunneling current peak which corresponds to tunneling from the emitter into the first quasibound state in the conduction band of the GaAs quantum well. The biases are not corrected for the effects of contact-series resistance, which we estimate to be less than 2 Ω. Symmetric diodes $S1$ and $S2$ show approximately symmetrical I-V characteristics under positive and negative biases, with peaks in

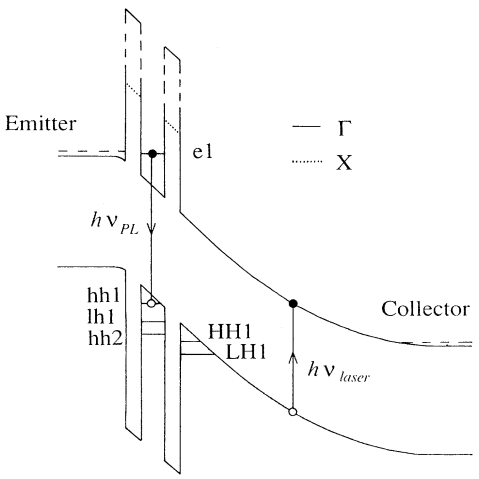

FIG. 1. The schematic of a double-barrier structure with applied bias showing Γ-band profiles and lowest quasibound-state energies in the well and collector. Dotted lines indicate the X-valley conduction band in the barriers. Horizontal dashed lines indicate Fermi levels in the heavily doped emitter and collector contacts.

the current near $V_P = \pm 0.65$ and ± 0.3 V, respectively. Increasing the barrier thicknesses from 2.5 nm in diode $S1$ to 5.1 nm in $S2$ reduces the peak tunneling current by more than three orders of magnitude. Asymmetric diode $A1$ resembles diode $S1$ (2.5-nm barriers) when biased such that its emitter barrier is 2.5 nm wide and $S2$ (5.1-nm barriers) when biased such that its emitter barrier is 5.1-nm wide. This demonstrates that the electron-tunneling current depends primarily on the thickness of the emitter barrier in our devices, as discussed further in Sec. IV B. For the asymmetric diodes, we define forward bias as that giving the largest electron-tunneling current; this corresponds to the emitter barrier being the thinner of the two. There is no resonant-tunneling peak in $A1$ in reverse bias, but a feature can be detected in the second derivative characteristic at -0.50 V, where the resonance might be expected (a resonant-tunneling current of ~ 1 μA can be inferred). Diode $A2$ exhibits similar behavior to $A1$, but with a smaller degree of asymmetry, as expected. Bistability and hysteresis due to circuit effects are present for the larger ($\sim$mA) but not for the smaller ($\sim\mu$A) tunneling currents. Data from diodes $S1$ and $A1$ will be discussed in the most detail, and that from diodes $S2$ and $A2$ introduced only in order to emphasize certain points.

III. RADIATIVE RECOMBINATION

A. PL mechanism and PLE measurements

In this section, we discuss the relationship between the luminescence and transport. In the simplest model of steady-state radiative recombination, the (spectrally integrated) luminescence intensity $I_{\rm PL}$ from the quantum well is proportional to

$$I_{\rm PL} = \frac{p}{1 + R_{\rm nr}/R_r} , \tag{1}$$

where p is the minority carrier (usually hole) sheet density in the well, $R_{\rm nr}$ is the minority carrier nonradiative decay rate (generally dominated by tunneling out of the well), and the radiative recombination rate R_r increases linearly with electron density n at low density but can saturate at high density when the Fermi energy becomes large compared with the thermal energy.

In general the sheet densities of carriers n,p consist of a component directly photoexcited in the well ($n_w = p_w$) and a component due to carriers tunneling from the emitter or collector contacts (n_e, p_c). The optically excited electron densities in the emitter and collector are so small as to have negligible effect on the electron transport and optical emission at the excitation power densities used in our experiments. In contrast, holes photoexcited in the collector play a major role in determining recombination in the well and, at high illumination intensities, the current. Such holes accumulate in the lowest subband of the triangular potential well in the spacer region adjacent to the collector barrier (HH1 in Fig. 1) with two effects. First, they can tunnel into quasibound valence-band states in the well and supplement (with density p_c) those directly excited. There they can recombine with electrons directly (optically) or indirectly (electrically) injected. Second, the electric field in the collector is screened and more bias is dropped across the well and barriers than in the dark; the tunneling current peak is therefore shifted to lower bias. The presence of the spacer layer and the relatively low collector doping density play an important role in allowing sizable hole populations to build up in the collector depletion region.[13]

PLE measurements were performed with the detection window in the spectral region corresponding to the transition between the lowest-energy ($n = 1$) bound states in the conduction and valence bands in the quantum well ($e1$ and hh1 in Fig. 1), which occurs near 1.630 ± 0.005 eV in diodes selected from the center of each wafer. Figure 2 shows representative PL and PLE spectra of diode $A1$ at various biases. The PL peak corresponds to recombination of carriers in the $e1$ and hh1 states of the well. At zero bias the near-band-edge PLE spectrum shows well-defined peaks corresponding to the heavy- and light-hole excitons in the well ($e1$-hh1, $e1$-lh1) together with the corresponding continua at higher energies. With increasing applied bias a background spectrum develops which has a cutoff near 1.52 eV, below the threshold for absorption in the well, and which roughly mirrors the expected absorption spectrum of the n-type emitter and collector layers. The presence of this background confirms that the density of holes in the well is partly governed by photoexcitation of the collector and subsequent tunneling of holes into the well through the collector barrier.[9,13,16] In diode $A1$, in reverse bias (e.g., Fig. 2, -0.40 V), where the collector barrier is relatively thin, this indirect carrier creation process is more important than direct photoexcitation in the well, and the features in the PLE spectrum specific to the well are lost against a large background. In forward bias, excitation of the well

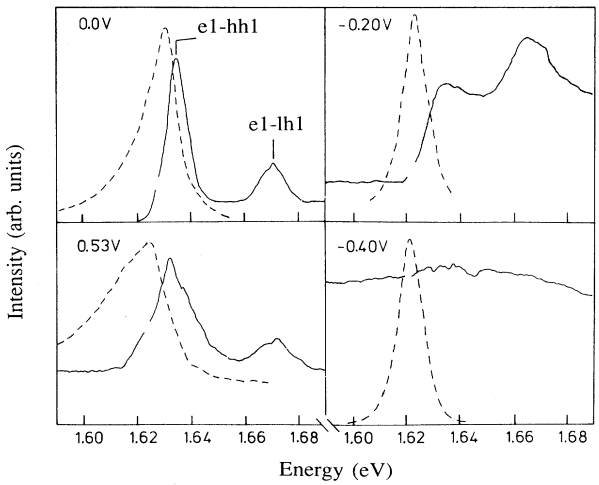

FIG. 2. PLE (solid curve) and PL (dashed curves) spectra of diode $A1$ at various biases recorded with a photoexcitation intensity of 10 W cm^{-2}. Parts of the solid curves corresponding to laser scans over the detection energy have been removed for clarity. The horizontal axis in each plot corresponds to the dark background.

and collector are of comparable importance. These PLE measurements demonstrate that, especially for the devices with a relatively thin collector barrier (diode $S1$, or $A1$ under reverse bias), the time-integrated intensity of PL from the well is strongly dependent on the hole-tunneling current as well as the electron current and lifetimes in the well. The PLE spectra also contain information on the free-carrier densities in the well. For example, at -0.20 V the heavy-hole peak shape in Fig. 2 is considerably modified and its center of gravity blueshifted relative to zero bias, indicating substantial heavy-hole accumulation. These effects are discussed further in Sec. IV A.

B. PL measurements

We begin our discussion of the PL measurements by describing data obtained under a sufficiently low intensity of photoexcitation (10 mW cm^{-2}) that there is negligible perturbation of the electronic I-V curves. Figures 3(a) and 3(b) show the dependence of the spectrally integrated luminescence intensity (over 3–6-meV bandwidth) and of the current on bias for diodes $A1$ and $S1$. At zero bias, the PL intensity arises from carriers directly excited and recombining in the well and is relatively weak. The luminescence intensity close to zero bias shows a quadratic dependence on illumination intensity between 10 mW cm^{-2} and 10 W cm^{-2}, suggesting that the nonradiative population decay rate exceeds the radiative recombination rate and therefore that the luminescence intensity is limited by tunneling of photoexcited carriers out of the well ($R_r \sim n, I_{\rm PL} \sim pn/R_{\rm nr}, p \sim p_w, n \sim n_w$). Using the methods described in Sec. IV B, we calculate electron escape times of less than 200 ps for $S1$ and $A1$, while the radiative lifetime deduced from the time-resolved PL measurements of Tsuchiya, Matsusue, and Sakaki[23] and Jackson *et al.*[24] is greater (at least a few hundred ps), which lends support to our interpretation.

When diodes $A1$ and $S1$ are biased in such a way that the *collector* barrier is 2.5 nm thick (i.e., $A1$ reverse biased, $S1$ either polarity), similar behavior is observed in the PL-V curves even though the I-V characteristics, which are largely determined by the *emitter* barrier (Sec. IV B) are very different. With bias beyond the threshold for significant electron tunneling, the intensity of luminescence from the well increases markedly for both diodes, and an approximately linear dependence of the PL intensity on the excitation power is obtained. In this regime, the PL intensity is proportional to the product of the electron and hole densities in the well for small n. Except for thick collector barriers when $p \sim p_w$, the PL intensity is then proportional to the product of the electron- and hole-tunneling currents ($n \sim n_e \gg p \sim p_c$); carriers directly photoexcited in the well are of secondary importance ($p > p_w, n_w$), as demonstrated by the PLE measurements. The electron-tunneling current and accumulation are not significantly perturbed by illumination, whereas all holes are photoexcited. At a given bias under weak illumination, n is fixed and the PL intensity is proportional to p, the density of holes in the well, and therefore to the excitation intensity. The similarities between the PL-V and I-V curves in Fig. 3(b) show that the hole-tunneling current has a relatively weak dependence on bias in the region of the electron-tunneling peak. This is because at very low illumination intensity, corresponding to small hole accumulation densities in the collector spacer, the hole distribution function is nondegenerate and no sharp tunneling features are expected, in contrast to the case where the hole population is degenerate. For large n_e, when the electrons in the well are degenerate, the radiative recombination rate becomes independent of n and the PL intensity is then proportional only to the

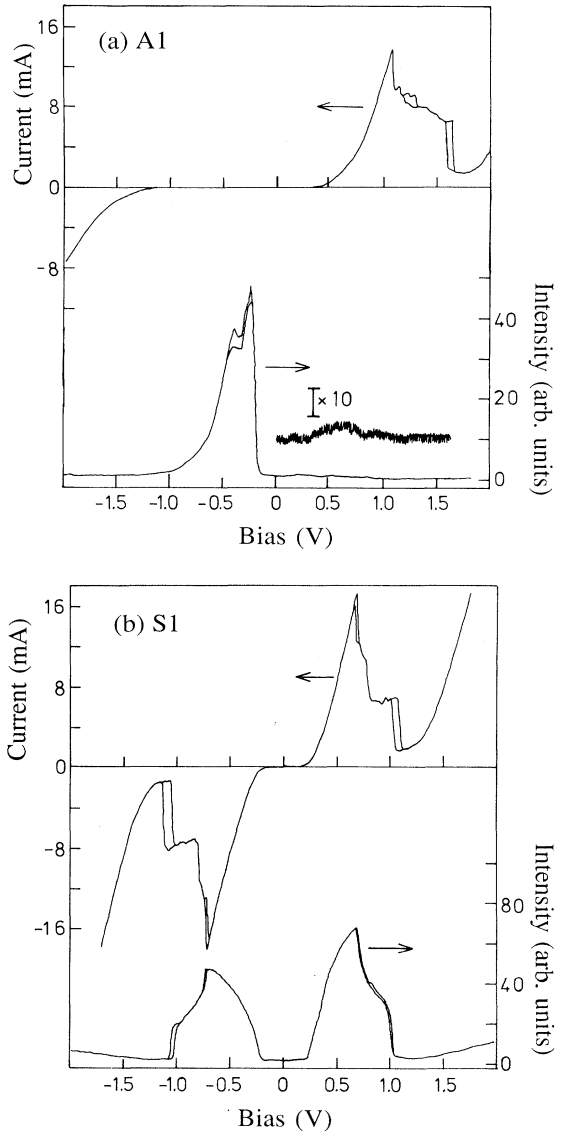

FIG. 3. I-V and PL-V characteristics of diodes (a) $A1$ and (b) $S1$ under low-intensity (10-mW cm^{-2}) photoexcitation at 1.81 eV. Hysteresis (probably a circuit effect) is observed in the regions of NDC, the higher-bias part of the curve corresponds to ramping the voltage up and the lower to ramping down. A common intensity scale is used for Figs. 3–6.

hole-tunneling current through the collector barrier. For large n_e, it is also possible for R_r to be greater than R_{nr} with the same result. These factors may explain why the PL intensity increases more slowly than the current with increasing bias on approaching the tunneling peak. In diode $A1$ some structure due to hole tunneling is observed in the PL-V, curve which is discussed further below.

When the devices are biased well above the peaks in the electron-tunneling current in Figs. 3(a) and 3(b), the total current increases while the luminescence intensity remains relatively low. This is due to several factors, the most important of which is the decrease in electron and hole dwell time (increase in R_{nr}) with increasing bias. Other effects include a reduction in the size of the matrix elements entering into the radiative recombination rate as the degree of electron-hole wave-function overlap is reduced with increasing field, and the possibility that for very large bias hot holes can be injected straight over the collector barrier without accumulating in the collector spacer.

In contrast to the behavior in reverse bias, in forward bias, where the collector barrier in $A1$ is twice as thick as in $S1$ and the emitter barriers are the same, the I-V characteristics are similar, whereas the PL-V curves are very different. The PL intensity in diode $A1$ is very weak and shows only a small change over the region of the peak in the electron-tunneling current. The PL intensity is mainly determined by holes directly excited in the well, suggesting that at the high electron densities achieved in this device the PL intensity becomes independent of n_e and instead $I_{PL} \sim p, p \sim p_w > p_c$. Figures 3(a) and 3(b) therefore demonstrate the importance of the current of holes tunneling through the collector barrier in determining the intensity of PL from the well.

Under intense photoexcitation (100 W cm^{-2}), the accumulation and tunneling of photoexcited holes is even more clearly revealed in the I-V and PL-V characteristics [Figs. 4(a) and 4(b)]. Assuming a carrier lifetime of order 100 ps (see Sec. III C), this intensity corresponds to a directly photoexcited carrier density in the well of less than 10^9 cm^{-2}, which is relatively small compared with the electrically injected electron density near the peak in the tunneling current, but the I-V and PL-V characteristics are nevertheless strongly modified by photoexcitation. The electron-tunneling peak occurs at lower bias under illumination than in the dark ($V_p = 0.54$ V under illumination and 1.10 V in the dark for $A1$, $V_p = 0.64$ and 0.70 V for $S1$, with device-to-device variations of ± 0.02 V). This effect is due to screening of the field in the collector depletion region by photoexcited holes, and is most pronounced for the devices with the thickest collector barriers ($A1$ and $A2$ in forward bias, $S2$ in either polarity), where the hole-tunneling probability through the collector barrier is smaller and a larger hole population can build up in the collector spacer. From the change in V_P with illumination, we calculate a collector spacer sheet charge density of $\sim 6 \times 10^{11}$ cm^{-2} for diode $A1$ and $\sim 1.5 \times 10^{11}$ cm^{-2} for $S1$ for biases near that of the peak electron-tunneling current. At these densities only the lowest-energy valence subband in the collector (HH1 in Fig. 1) is occupied, assuming quasithermal carrier statistics.

With increasing reverse bias, the PL intensity increases and exhibits maxima [features a and b in Figs. 4(a) and 4(b)] at the same biases as features in the I-V curve. These features are due to peaks in the hole-tunneling current which become clear at illumination intensities large enough to produce a degenerate hole population in the collector spacer, and are sufficiently large to contribute noticeably to the total current. Under low-intensity excitation the peaks in the PL-V curve are weaker because $p \sim p_w$. At feature a (0.42 V in $S1$, 0.37 V in $A1$) there is a distinct peak which we attribute to tunneling of heavy holes from HH1 collector states into the second heavy-hole level (hh2) in the well. This assignment is roughly supported by calculations of the band lineups (as indicated in Sec. II and using the hole masses suggested

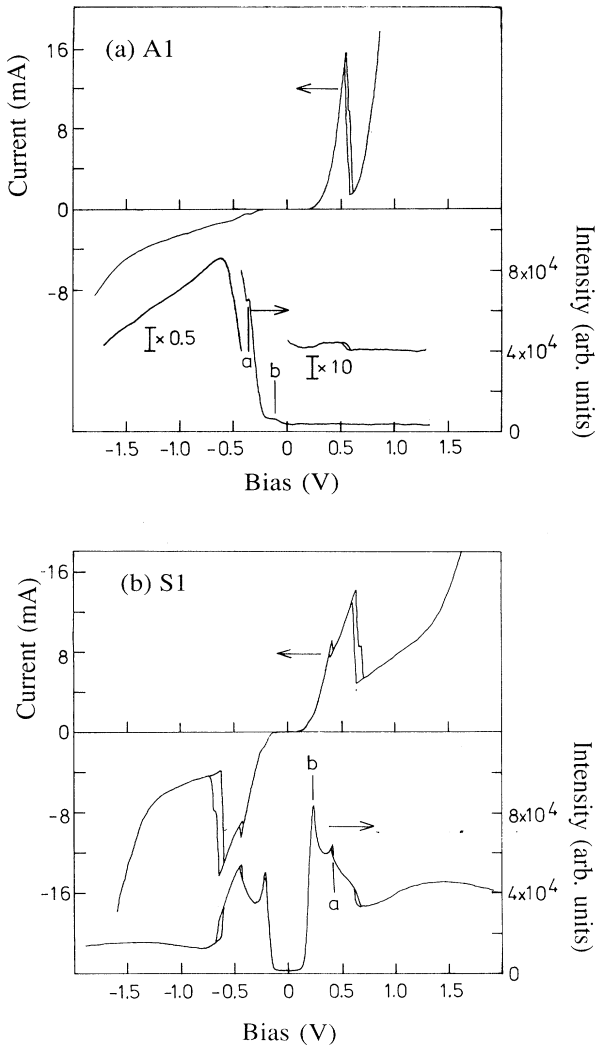

FIG. 4. I-V and PL-V characteristics of diodes (a) $A1$ and (b) $S1$ under high-intensity (100-W cm^{-2}) photoexcitation at 1.81 eV.

by Miller and Kleinman[25]). In the dark we calculate a peak HH1-hh2 current at 0.35 V in $S1$ and 0.30 V in $A1$. We estimate that these biases would be 10% or 20% smaller under illumination. In both diodes, the bias for peak HH1-hh1 tunneling is calculated to occur at less than 0.05 V and thus lies below the threshold for electron tunneling. In addition, at low bias there is relatively little hole accumulation because of the moderately high collector doping.[13] Taken together these factors may explain why there is not a noticeable peak in either the PL-V or I-V characteristics for this tunneling process. At feature b (0.24 V in $S1$, 0.14 V in $A1$) there is a maximum (diode $A1$) or shoulder (diode $S1$) in the tunneling current, which we attribute to tunneling from HH1 into the lowest light-hole level in the well (lh1). We calculate that this should occur at 0.23 V in $S1$ and 0.20 V in $A1$ in the dark, which supports our assignment. This tunneling process requires band mixing, which is mentioned again in Sec. III C.

Figure 5, which combines information contained in the PL-V and I-V curves in Figs. 4(a) and 4(b), shows the variation of PL intensity with current. For the asymmetric device in forward bias, the PL intensity is low and nearly independent of current, as discussed above. In reverse bias the PL intensity is accurately linear with current up to the PL maximum at -0.6 V. Over this range of bias in the absence of photoexcitation, the electron current is extremely small, but with increasing photoexcitation intensity the current increases strongly. We suggest that in this geometry the total current is determined by the current of holes through the collector barrier. The density of holes confined in the well increases, increasing the potential drop across the emitter barrier, until a steady state is achieved in which the currents of electrons through the emitter and holes through the collector are equal both to each other and to the rate of recombination in the well. The current of holes out of the well through the wide emitter barrier is negligible. The hole accumulation in the well causes a reduction in band gap and a shift in PL energy; these effects are discussed in Sec. IV A. For diode $S1$, the PL intensity is approximately proportional to current for small biases (up to luminescence peak b) for similar reasons. At higher biases the hole current through the collector barrier is smaller than the electron current through either barrier, and the current of holes escaping from the well through the emitter barrier may be significant. There is therefore no simple relationship between the hole current, the total current, and the recombination rate.

The evolution of the I-V and PL-V characteristics with decreasing illumination intensity generally takes place smoothly, as illustrated by the behavior in diode $S2$ shown in Fig. 6. In this device, hole tunneling is particularly clear in the PL-V characteristics at 1 W cm^{-2} [Fig. 6(c)], with a sharp, well-resolved tunneling peak at 0.17 V and valley near 0.25 V. The tunneling peak is only 24 mV wide, corresponding to an energy width of 12 meV which is comparable to the estimated heavy-hole Fermi energy in the collector spacer required to give the observed 0.05-V shift in the bias of the electron-tunneling peak with illumination. NDC has also been observed, although less clearly, in hole transport in p-type DBTD's.[26–28] We identify the dominant sharp peak in the PL-V characteristic [Figs. 6(c) and 6(d)] with HH1-lh1 tunneling, and the small peak evident near 0.29 V in Fig. 6(b) with HH1-hh2 tunneling. The calculated biases for HH1-hh2 and HH1-lh1 peak tunneling currents, neglecting hole accumulation in the collector spacer, are 0.29 and 0.20 V, respectively, consistent with the peak positions in Fig. 6. Behavior resembling that shown in Figures 6(c) and 6(d) has been observed in the electro-

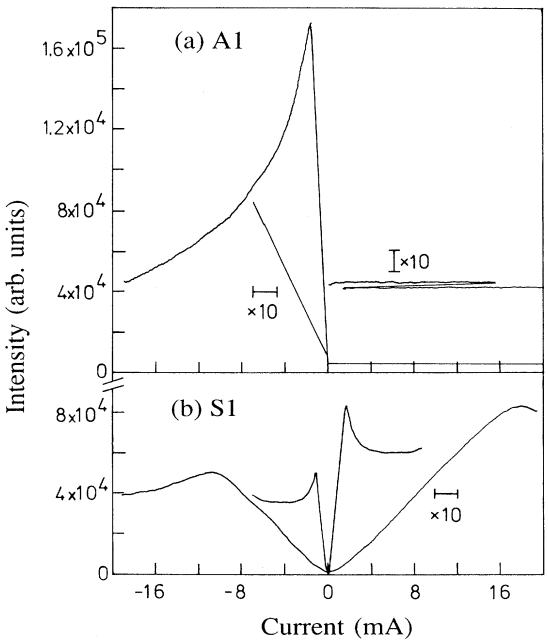

FIG. 5. PL-I characteristics of diodes (a) $A1$ and (b) $S1$ under high-intensity (100-W cm^{-2}) photoexcitation at 1.81 eV.

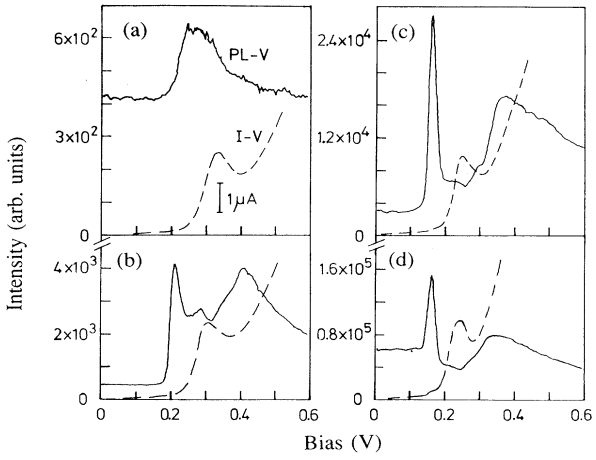

FIG. 6. PL-V spectra of diode $S2$ under different 1.65-eV excitation power densities (a) 10 mW cm^{-2}, (b) 100 mW cm^{-2}, (c) 1 W cm^{-2} and (d) 100 W cm^{-2}. Dashed curves indicate I-V characteristics.

luminescence intensity of a structure similar in important respects to $S2$, except for the fact that the collector was p type.[18] The emission in this case was attributed to $e1$-lh1 recombination and led the authors of Ref. 18 to conclude that a population inversion between hh1 and lh1 states had been achieved in their device. In our structure, the recombination is unambiguously identified by PLE measurements as $e1$-hh1, and we have not found any evidence of $e1$-lh1 emission.

For illumination intensities lower than 100 mW cm^{-2}, the photoexcited hole population in the collector spacer is no longer degenerate, and sharp tunneling features cease to be evident, as shown in Fig. 6(a). The PL-V behavior of diode $S2$ might be expected to resemble $A1$ in forward bias, where the collector barriers are similar. The fact that hole-tunneling peaks are observed in the PL-V characteristics of diode $S2$ but not $A1$ in forward bias suggests that $p_c \sim p_w$ in $S2$, whereas $p_c < p_w$ in $A1$ because of the thicker emitter barrier in the former which favors hole accumulation in the well.

Whereas the behavior seen in Fig. 6 and also in diodes $A1$ and $A2$ is what might be expected with increasing hole population in the collector, the behavior in diode $S1$ is more complicated. With decreasing illumination intensity the bias of feature a in the high-intensity plot in Fig. 4(b) (attributed to HH1-hh2 tunneling) increases in such a way that at low intensity the electron-tunneling peak occurs first. This behavior is not presently understood.

C. Pulsed excitation

Time-resolved PL measurements on diodes $S1$ and $A1$ confirm the importance of hole tunneling from the collector into the well in determining the PL intensity. Figure 7 shows streak camera traces of the evolution of the PL from the well in diodes $S1$ and $A1$ following excitation by 1-ps pulses at 1.84 eV. Such measurements were performed in the high-intensity photoexcitation regime (100 W cm^{-2} average power). At zero bias the PL decay time is approximately 200 and 100 ps in $S1$ and $A1$, respectively; the rise time is not resolved (<30 ps). This PL is due to carriers directly excited in the well and, as argued in Sec. III B, its decay is strongly influenced by carriers tunneling out of the well.

In diode $A1$, the PL decay time is approximately independent of forward bias. In diode $S1$, and in diode $A1$ in reverse bias, a long-lived component develops and is seen as a steady level at later times. The long-lived PL component is due to the current into the well of holes photoexcited in the collector, and has maximum intensity at the bias corresponding to the peak time-integrated intensity [Figs. 4(a) and 4(b)]. The electron population in the well at later times is provided by carriers tunneling from the emitter. The rapidly rising and decaying components of the PL show maxima in intensity at lower values of bias near features a in Figs. 4(a) and 4(b), which we have attributed to HH1-hh2 tunneling. This suggests that the decay of the directly excited carrier population is also influenced by holes tunneling from the collector.

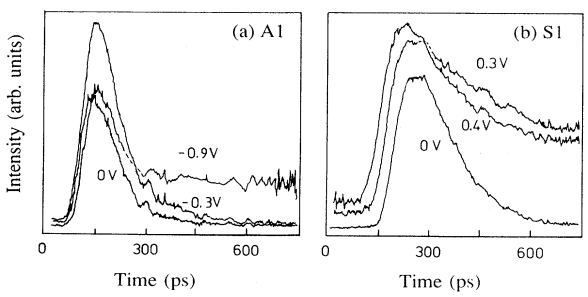

FIG. 7. Time-resolved PL spectra from diodes (a) $A1$ and (b) $S1$ at various biases with excitation (100 W cm^{-2}) at 1.81 eV. The horizontal axis corresponds to the dark background.

For instrumental reasons we were unable to determine the characteristic decay time of the long-lived component, but can place a lower limit of a few ns and an upper limit of ~ 10 ns upon it. The rise time of this long-lived component is at most 3–400 ps. To describe the behavior of the long-lived component, we consider a simple model of the kinetics in which a hole population is instantaneously created in the collector spacer by the laser pulse. In effect we are assuming that holes excited elsewhere in the collector drift to the spacer region on a relatively short-time scale, on the order of a few hundred ps or less, which is reasonable since a hole can drift more than 100 nm in this time for typical fields. This hole population can then decay, with time constant τ_c, by tunneling into the well and by recombination in the vicinity of the collector spacer. A rate equation analysis shows that the rise time of the PL due to holes tunneling from the collector is determined by the shorter, and the decay time by the longer, of τ_c and the lifetime of holes in the well, τ_w. From our zero-bias measurements, we estimate that τ_w is a few hundred ps or less, so that the rise time of the long-lived component is determined by τ_w (and to a lesser extent by the drift of holes over the length of the collector), and the decay time by the shorter of the time constants for hole tunneling through the collector barrier and recombination in the collector spacer. A simple calculation of the heavy-hole tunneling time in diode $S1$ at an arbitrary bias of 0.3 V gives a result of ~ 1 μs, but light holes can tunnel much more rapidly than heavy holes, and the average hole tunneling time is very sensitive to band mixing and can be dramatically reduced by carrier density and heating effects.[29,30] Our results therefore only allow us to place a lower limit of a few ns on the average hole-tunneling time, in agreement with the results of Ref. 13.

IV. DETERMINATION OF ELECTRON DENSITY IN THE WELL

A. PL measurements

Figures 8(a) and 8(b) show the variation of PL energy and linewidth in diodes $A1$ and $S1$, and also the Stokes energy shift between the peak in the emission spectrum and the $n=1$ heavy-hole "excitonlike" feature in the PLE spectrum (Fig. 2). These measurements were made with an excitation power density of 10 W cm^{-2}, which is

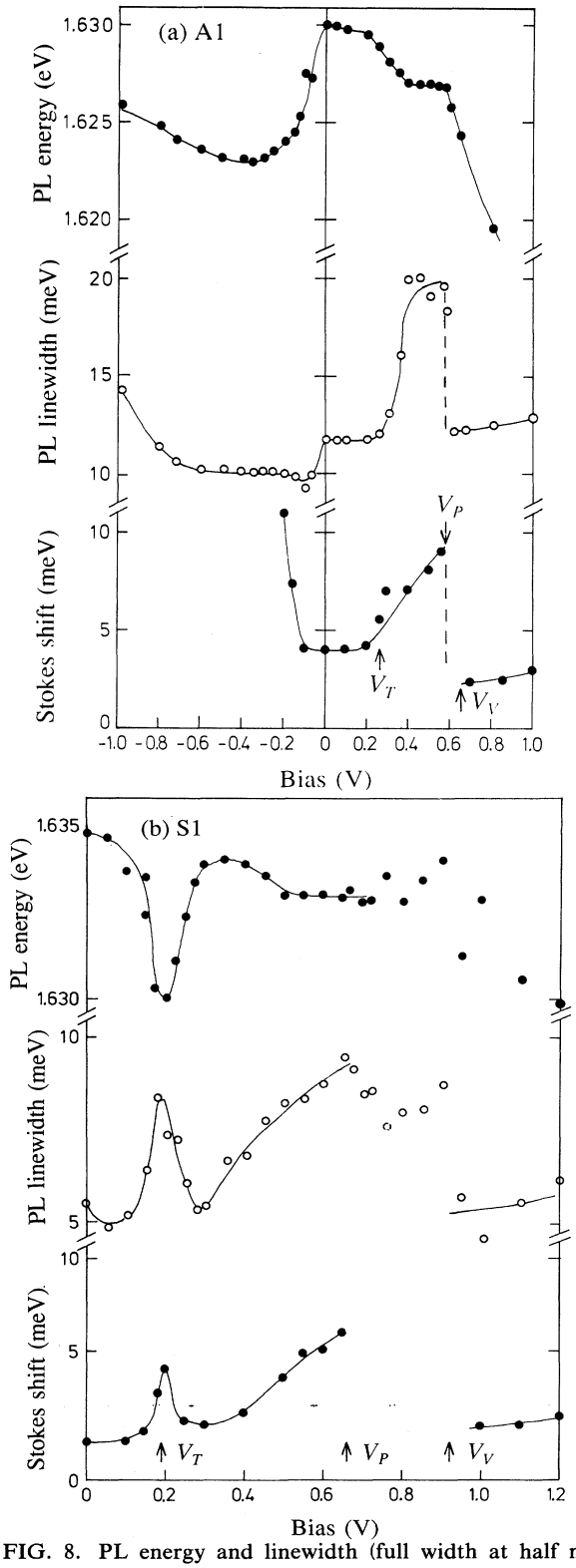

FIG. 8. PL energy and linewidth (full width at half maximum) and Stokes shift between peaks of PL and PLE as a function of bias for diodes (a) $A1$ and (b) $S1$. The photoexcitation intensity was 10 W cm^{-2} at 1.65 eV. V_P, V_T, and V_V indicate approximate biases of the threshold, peak, and valley of the tunneling current. Dashed lines indicate regions of circuit instability, where the device state is not well defined.

a factor of 10 lower than in the high-excitation regime described above. All three quantities contain information about carrier accumulation in the well, but the clearest picture of charge buildup is given by the Stokes shift. There is a 4-meV Stokes shift at zero bias and low temperature which can be attributed to exciton localization effects. Under bias, the band-filling effect of free carriers gives rise to a further increase in Stokes shift with increasing carrier density:

$$\delta E_{\rm SS} = \frac{\pi\hbar^2}{\mu} n \ , \tag{2}$$

where μ is the reduced "exciton" mass. From the change in Stokes shift of 7 meV between peak and valley observed in diode $A1$ [Fig. 8(a)], and using $\mu = 0.05 m_0$,[31] Eq. (2) gives a change in carrier density of $n = 1.5\times10^{11}$ cm^{-2}. We thus deduce an electron sheet density at the peak of the tunneling current of this magnitude. Similarly, for diodes $S1$ [Fig. 8(b)], $A2$, and $S2$, we obtained $n \sim 7.5\times10^{10}$, $n \sim 1.1\times10^{11}$, and $n < 2\times10^{10}$ cm^{-2}, respectively. Measurements made under lower-intensity (100 mW cm^{-2}) photoexcitation gave similar results. For diode $A1$ in reverse bias, Fig. 8(a) shows evidence of charge buildup between 0 and -1 V, which we attribute to heavy-hole accumulation in the well. This is confirmed by the fact that the intensity of the $e1$-hh1 peak in the PLE spectrum (see Fig. 2, -0.2 V) is reduced relative to $e1$-lh1, the former being effected by heavy-hole band filling but not the latter. Note that the PL linewidth is smaller than that at 0 V. This is possibly because of the reduced importance of indirect transitions involving HH1 collector spacer states when the well contains a significant heavy-hole population. We were unable to measure the Stokes shift much beyond -0.2 V because of the large indirectly excited background in the PLE spectrum (see Fig. 2, -0.40 V); we estimate a hole population $p_c \sim 10^{11}$ cm^{-2} at this point. The behavior of the electron density indicated by the Stokes shift data for diode $S1$ in Fig. 8(b) is similar to $A1$ in forward bias, but there is also a significant hole population in the well of diode $S1$ near 0.20 V. Using Eq. (2), we estimate that the peak value of p_c is $\sim 5\times10^{10}$ cm^{-2}.

The PL energy and line shape also contain information about charge accumulation in the well, but analysis is generally more complicated. Both many-body effects (band-gap renormalization) and changes in the single-particle energy due to the change in shape of the potential profile in the quantum well contribute to the variation in PL energy with bias. The largest single-particle contribution is generally from the Stark shift, which depends on the distribution of charge in the device and is not a simple function of applied bias in the region of the electron-tunneling peak. The magnitude of the band-gap renormalization may be estimated using an interpolation formula derived by Schmitt-Rink and Ell[32] in a two-dimensional (2D), zero-temperature random-phase approximation which, for the change in PL energy, gives

$$\delta E_{\rm PL} = \delta E_s - 3.1 \left[\frac{n a_0^2}{2}\right]^{1/3} E_s \ , \tag{3}$$

where a_0 is the Bohr radius and δE_s is the change in the exciton binding energy. This expression has previously been found to provide a reasonable description of band-gap renormalization in indirectly populated (i.e., not directly doped) quantum wells[33,34] with the substitution of effective quasi-2D parameters. The exciton binding energy becomes very small at modest carrier densities,[35] so that we can take $\delta E_s \sim E_s$. Using effective parameters appropriate to a 5-nm quantum well ($a_0 \sim 10$ nm, $E_s \sim 10$ meV), we then obtain $\delta E_{\rm PL} \sim 2$ meV for an electron sheet density of 1×10^{11} cm^{-2}, which is similar in magnitude to the Stark shift expected at this bias and to the step in PL energy in diode $A1$ between 0.2 and 0.6 V in Fig. 8(a). This illustrates the difficulty of separating the contribution of many-body effects from the overall variation in PL energy.

In forward bias there is an increase in linewidth of 8 and 4 meV in diodes $A1$ and $S1$, respectively, between the tunneling current threshold and peak biases. This is due partly to free-carrier broadening of order E_F and partly to a low-energy tail which develops further with increasing forward bias, as can be seen in Fig. 2. Free-carrier broadening should lead to an increase in emission at energies higher than the peak. One possible explanation for the low-energy emission is that it is associated with an indirect transition between the $e1$ state in the well and the HH1 state in the collector spacer, with energy close to but lower than the hh1 level in the well. To estimate the Fermi level, we might consider only the variation in the half-width from the luminescence peak to the half-height point on the high-energy side, in which case we find that the width increases by 3 meV, which is similar to that expected for a sheet carrier density of order 10^{11} cm^{-2}. On the other hand, there is a decrease in both the full width and half-width in diode $A1$ on going from 0 to -0.2 V, while the Stokes shift data suggest a buildup of holes, thus showing that any such simple analysis of the PL line shape is doubtful. The complicated spectral shape of the PL makes it difficult to extract information from a line-shape analysis about the change in Fermi level in the well with bias.

B. Discussion

In this section, we discuss the measured peak tunneling currents and charge buildup in the well using the sequential tunneling description of the DBTD, and relate these two quantities to the time taken for an electron to tunnel through the collector barrier. In this model we can express the current density at low temperature, where thermionic emission is negligible, in the form

$$J \approx \frac{e\sqrt{mE_0/2}}{2\pi\hbar^2 L_w}(E_F - E_z)\frac{T_e T_c}{T_e + T_c} , \tag{4}$$

where T_e, T_c are the emitter and collector barrier transmission probabilities for electrons with energy matched to that of the bound state in the well, L_w is the well width, E_F is the Fermi level in the emitter spacer, m is the electron mass in the well, and E_z is related to the bound-state energy in the well (E_0), and potential drops across emitter barrier and well, ($V_{\rm eb}, V_w$), by $E_z = E_0 - eV_{\rm eb} - eV_w/2$. All energies are measured relative to the bottom of the GaAs conduction band. We have assumed that the energy width of the bound state in the well is smaller than the width of the energy distribution in the emitter, and that tunneling preserves the in-plane-wave vector. Equation (4) is approximately equivalent to that derived in a coherent tunneling model and remains unchanged to first order in the presence of weak scattering (defined below). In the limit that the transmission coefficients of the two barriers are very different, the model predicts that the current is determined by the more opaque barrier. Hence, for the symmetric diodes and the asymmetric diodes under reverse bias, we expect that $T_c > T_e$, and that J is proportional to T_e. For asymmetric diodes under forward bias, $T_c < T_e$, and J is proportional to T_c.

For the transmission coefficient of a single barrier as a function of energy E, we use the Wentzel-Kramers-Brillouin approximation modified by the inclusion of a prefactor obtained by extending the exact flat-band result[36] to first order in the potential drop V_b across the barrier:

$$T(E,V_b) \simeq \frac{16rc\sqrt{E(E+eV_b)}(V_0 - E_0)}{[(V_0 - E_0)r + E][(V_0 - E_0)r + E + eV_b]} \times e^{-2\int_0^{L_b} k_b dz} , \tag{5}$$

where V_0 is the barrier height, r is the ratio of electron mass in the barrier to that in GaAs, and k_b is the perpendicular wave vector in the barrier. We take into account the fact that tunneling takes place far from the AlAs Γ band edge by using an approximate energy-dependent Γ effective mass $m_b(E) = m_b(V_0)[(1-(V_0-E)/E_w)]$, with $E_w = \hbar^2/2m_b(V_0)\gamma$, and γ calculated in a five-band model is 9.8×10^{-20} m^2.[37]

The charge density is related simply to the current density in the quantum well by a dwell time $\tau = n/J$, which describes the decay of charge through the collector barrier[18]:

$$\tau = \frac{2L_w\sqrt{m/2E_0}}{T_c} . \tag{6}$$

Using transmission coefficients calculated considering only transport in the Γ valley, Eq. (4) describes the magnitude of the peak tunneling current in the symmetric diodes and reverse-biased asymmetric diodes reasonably well, as can be seen by comparing the experimental and theoretical values in Tables I and II, especially when account is taken of the uncertainty in sample and materials parameters and the fact that our treatment probably underestimates the tunneling current by a factor of order two or three compared with a self-consistent calculation.[38] In contrast, the predictions of the theory are not borne out by the results on either asymmetric diode in forward bias. In particular the measured peak tunneling current in $A1$ is very close to that in $S1$, suggesting that J is proportional to T_e rather than to T_c, as predicted.

TABLE II. Peak tunneling currents calculated in the sequential model together with measured (using $\tau^f = n/J_P^f$) and calculated tunneling times through the collector barrier in forward bias. Unstarred calculations are for tunneling in Γ valleys only, starred calculations include parallel X-valley tunneling with the branching ratio $c_{\Gamma X} = 1 \times 10^{-4}$. N_D is taken as 2.5×10^{17} cm^{-3} in $A1$, $A1$, and $S2$, and 5×10^{17} cm^{-3} in $A2$.

Diode	I_P^f (calc.)	I_P^r (calc.)	τ^f (calc.)	τ^f (meas.)
$S1$	2.6 mA	2.6 mA	80 ps	80 ps
$S1^*$	2.7 mA	2.7 mA	58 ps	
$A1$	12 μA	0.23 μA	390 ns	170 ps
$A1^*$	2.7 mA	1.2 μA	260 ps	
$A2$	16 μA	0.48 μA	480 ns	1.9 ns
$A2^*$	0.21 mA	2.7 μA	730 ps	
$S2$	0.23 μA	0.23 μA	670 ns	<90 ns
$S2^*$	1.2 μA	1.2 μA	2.3 ns	

Values of τ calculated near the peak in the tunneling current using Eq. (6) are compared with n/J obtained from the Stokes shift and transport measurements in Table II. This comparison is more telling, since the calculated value of τ, unlike J, is only weakly dependent on the crudely modeled charge distribution in the emitter. The agreement is again satisfactory for the symmetric diode $S1$ and for the asymmetric diodes in reverse bias, but not for the forward-biased asymmetric diodes or for diode $S2$. For example, for diode $A1$, τ is overestimated by a factor of ~2300. We interpret this discrepancy between theory and experiment as due to the neglect of scattering. In the theory of Bar-Joseph and Gurvitz,[7] scattering in the well can be included in the framework of Eqs. (4)–(6) by replacing T_c with $T_c + T_i$, where T_i is the scattering rate divided by an attempt frequency $(2E_0/m)^{1/2}/2L_w$. In asymmetric diodes, for which $T_c < T_e$, the current is expected to be different in the weak ($T_i \ll T_c, T_e$) and strong ($T_i \gg T_c, T_e$) scattering limits. The strong-scattering model predicts that J is proportional to T_e for both $T_c > T_e$ and $T_e > T_c$, in contrast to the predictions of the weak-scattering or coherent models where J is proportional to the smallest transmission coefficient. Strong scattering can therefore explain the large peak tunneling current observed in diodes $A1$ and $A2$. The qualitative predictions of the model do not depend on the microscopic details of the scattering mechanism. Bar-Joseph and Gurvitz considered irreversible scattering in the well, whereas the indirect band-gap structure of the AlAs barriers in our structures suggests a different mechanism in which the transparency of the barriers is enhanced by scattering into X-point conduction-band valleys. This would explain the short dwell times observed in diodes $A1$ and $A2$.

Transport measurements[39,40] demonstrate that the effective height of a single AlAs barrier for tunneling, and thermionic emission is closer to the GaAs-AlAs Γ-X conduction-band offset $\Delta E_{X\Gamma} \sim 0.2$ eV (Ref. 41) than to the Γ-Γ offset $\Delta E_{\Gamma\Gamma} \sim 1.05$ eV, thus showing the importance of intervalley scattering.[20,39,40,42] Experimentally the mass appearing in the exponent of Eq. (5) is generally found to be much closer to the small transverse X_t mass $m \sim 0.2 m_0$ than to the large longitudinal X_1 mass $m \sim 1.1 m_0$,[43] suggesting that scattering into X_t valleys is the most important process even though tunneling via X_1 valleys can occur without scattering because of the broken symmetry of the lattice in the growth direction. This hypothesis is supported by empirical pseudopotential calculations,[44] which suggest that tunneling via X_1 valleys is only relatively weakly favored compared with that in the Γ valley. Tunneling involving the X point has been used to explain the pressure dependence of the valley currents in AlAs/GaAs/AlAs DBTD's,[20,21] but the magnitude of the peak tunneling current in symmetric GaAs/AlAs DBTD's was previously thought to be determined by the Γ offset of the emitter barrier.[19,29,45] We suggest that tunneling via the X point is important in determining both the peak and valley currents in the general case.

The relative contributions of the Γ and X tunneling processes depend not only on the transmission coefficients T_Γ, T_X associated with evanescent states in the different valleys but also on the scattering rate between the Γ and X valleys which we describe by a branching ratio $c_{\Gamma X}$, defined such that the total transmission coefficient through a single barrier is $(1 - c_{\Gamma X})T_\Gamma + c_{\Gamma X} T_X$ ($c_{\Gamma X} T_X$ is similar to T_i in the notation used above). The dwell time data for diodes $A1$ and $A2$ can be reasonably well described (to within a factor of order 2) by taking $c_{\Gamma X} = 1 \times 10^{-4}$ for both barriers, a value also consistent with the data on the symmetric diodes (Table II). For this value of $c_{\Gamma X}$, transport in the X_t valleys dominates that in the Γ valley for barrier widths greater than about 3 nm. The peak tunneling current in the symmetric diode $S1$ is dominated by Γ valley tunneling processes, whereas tunneling via X_t valleys dominates in all the other diodes and is clearly incoherent. The relative proportions of Γ and X tunneling may depend on the nature and density of impurities in the barriers and on the roughness of the interfaces and so be sample dependent,[46] but a value for $c_{\Gamma X}$ of order 10^{-4} is consistent with measurements of effective Richardson constants made on indirect GaAs/Al_xGa_{1-x}As single-barrier tunneling structures by Solomon, Wright, and Lanza[39] and Kyono *et al.*[40] It is interesting to note that calculations of elastic Γ-X_t scattering by alloy potential fluctuations in $Al_{0.5}Ga_{0.5}As$ single barriers[47] show order-of-magnitude agreement with our experimental estimate of $c_{\Gamma X}$. This may not be a coincidence, since roughness of the GaAs/AlAs interface must impart to it some characteristics of the alloy, although it is possible that inelastic scattering involving phonons also plays a part.

V. SUMMARY

The optical emission from the quantum wells in photoexcited AlAs/GaAs/AlAs DBTD's has been investigated and correlated with transport measurements. Photoexcited holes accumulate in the collector spacer and from there tunnel into the $n = 1$ light-hole and $n = 2$ heavy-hole levels in the quantum well, where they can relax to the $n = 1$ heavy-hole level and play a major role in determining the intensity of recombination with $n = 1$ electrons. Since the intersubband relaxation time is typi-

cally much shorter than the dwell time in the well, the observed hole-tunneling processes are clearly incoherent. Under high-intensity illumination, resonant hole tunneling can be directly observed as peaks superimposed on the electron current-voltage characteristics. Under certain conditions the hole-tunneling current may control the current through the device.

By measuring the variation in the Stokes shift between emission and absorption, we have determined the electron sheet charge density in the well near the peak in the tunneling current and used this to deduce the average time taken for electrons to tunnel through the collector barrier. For AlAs barriers thicker than about 3 nm, this time is found to be shorter than expected for tunneling via Γ-valley evanescent states alone, but is consistent with the existence of a more efficient parallel tunneling process involving scattering into transverse X-valley states with a branching ratio of order 10^{-4}. Both the electron and hole tunneling take place in the strong-scattering (incoherent) regime, in which the current depends only on the transmission coefficient of the emitter barrier even for asymmetric diodes with very thick collector barriers; this behavior is quite different from that expected in a coherent model.

ACKNOWLEDGMENTS

One of us (S.R.A.) would like to acknowledge useful discussions with M. J. Kearney, and the Royal Society and Science and Engineering Research Council for financial support with which part of this work was carried out.

*Also at: Cavendish Laboratory, Cambridge CB3 0HE, United Kingdom.

†Present address: VG Semicon Ltd., Inberhorn Lane, East Grinstead, West Sussex RH19 1XZ, United Kingdom.

[1]E. E. Mendez, in *Physics and Applications of Quantum Wells and Superlattices,* edited by E. E. Mendez and K. von Klitzing, Vol. 170 of *NATO Advanced Study Institute Series B: Physics* (Plenum, New York, 1987), p. 159.

[2]M. L. Leadbeater, E. S. Alves, F. W. Sheard, L. Eaves, M. Henini, O. H. Hughes, and G. A. Toombs, J. Phys. Condens. Matter **1**, 10 605 (1989).

[3]I. Bar-Joseph, Y. Gedalyahu, A. Yacoby, T. K. Woodward, D. S. Chemla, D. L. Sivco, and A. Y. Cho, Phys. Rev. B **44**, 8361 (1991).

[4]S. Luryi, Appl. Phys. Lett. **47**, 490 (1985).

[5]T. Weil and B. Vinter, Appl. Phys. Lett. **50**, 1281 (1987).

[6]T. K. Woodward, D. S. Chemla, I. Bar-Joseph, H. U. Baranger, D. L. Sivco, and A. Y. Cho, Phys. Rev. B **44**, 1353 (1991).

[7]I. Bar-Joseph and S. A. Gurvitz, Phys. Rev. B **44**, 3332 (1991).

[8]J. Young, B. M. Wood, G. C. Aers, R. L. S. Devine, H. C. Liu, D. Landheer, and M. Buchanan, Phys. Rev. Lett. **60**, 2085 (1988); **62**, 1208 (1989).

[9]N. Vodjdani, F. Chevoir, D. Thomas, D. Cote, P. Bois, E. Costard, and S. Dalaitre, Appl. Phys. Lett. **55**, 1528 (1989).

[10]N. Vodjdani, D. Cote, D. Thomas, B. Sermage, P. Bois, E. Costard, and J. Nagle, Appl. Phys. Lett. **56**, 33 (1990).

[11]N. Vodjdani, D. Cote, F. Chevoir, D. Thomas, E. Costard, J. Nagle, and P. Bois, Semicond. Sci. Technol. **5**, 538 (1990).

[12]D. C. Hayes, M. S. Skolnick, P. E. Simmonds, L. Eaves, D. P. Halliday, M. L. Leadbeater, M. Henini, and O. H. Hughes, Surf. Sci. **228**, 373 (1990).

[13]S. Charbonneau, J. F. Young, and A. J. Spring Thorpe, Appl. Phys. Lett. **57**, 264 (1990).

[14]H. Yoshimura, J. N. Schulman, and H. Sakaki, Phys. Rev. Lett. **64**, 2422 (1990).

[15]M. S. Skolnick, D. G. Hayes, P. E. Simmonds, A. W. Higgs, G. W. Smith, H. J. Hutchinson, and C. R. Whitehouse, Phys. Rev. B **41**, 10 754 (1990).

[16]M. S. Skolnick, P. E. Simmonds, D. G. Hayes, A. W. Higgs, G. W. Smith, A. D. Pitt, C. R. Whitehouse, H. J. Hutchinson, C. R. H. White, L. Eaves, M. Henini, and O. H. Hughes, Phys. Rev. B **42**, 3069 (1990).

[17]I. Bar-Joseph, T. K. Woodward, D. S. Chemla, D. Sivco, and A. Y. Cho, Phys. Rev. B **41**, 3264 (1990).

[18]C. R. H. White, M. S. Skolnick, L. Eaves, M. L. Leadbeater, M. Henini, O. H. Hughes, G. Hill, and M. A. Pate, Phys. Rev. B **45**, 6721 (1992).

[19]M. Tsuchiya and H. Sakaki, Appl. Phys. Lett. **50**, 1503 (1987).

[20]E. E. Mendez, E. Calleja, and W. I. Wang, Phys. Rev. B **34**, 6026 (1986).

[21]R. Pritchard, D. G. Austing, P. C. Klipstein, J. S. Roberts, A. W. Higgs, and G. W. Smith, J. Appl. Phys. **68**, 205 (1990).

[22]S. R. Andrews, A. J. Turberfield, and B. A. Miller, Superlatt. Microstruct. **9**, 357 (1991). The sample parameters given in this preliminary account were those given in the growth specification and differ slightly from the measured values used in the present paper.

[23]M. Tsuchiya, T. Matsusue, and H. Sakaki, Phys. Rev. Lett. **59**, 2356 (1987).

[24]M. K. Jackson, M. B. Johnson, D. H. Chow, T. C. McGill, and C. W. Niels, Appl. Phys. Lett. **54**, 552 (1989).

[25]R. C. Miller and D. A. Kleinman, J. Lumin. **30**, 520 (1985).

[26]E. E. Mendez, W. I. Wang, B. Ricco, and L. Esaki, Appl. Phys. Lett. **47**, 415 (1985).

[27]T. Nakagawa, T. Fujita, Y. Matsumoto, T. Kojima, and K. Ohta, Appl. Phys. Lett. **50**, 974 (1987).

[28]C. Van Hoof, G. Borghs, and E. Gooverts, Appl. Phys. Lett. **59**, 2139 (1991).

[29]M. Nido, M. G. W. Alexander, and W. W. Ruhle, Appl. Phys. Lett. **56**, 355 (1990).

[30]D. Z. Ting, E. T. Yu, and T. C. McGill, Phys. Rev. B **45**, 3576 (1992).

[31]A. S. Plaut, R. T. Harley, S. R. Andrews, and T. M. Kerr, Phys. Rev. B **42**, 1332 (1990).

[32]S. Schmitt-Rink and C. Ell, J. Lumin. **30**, 585 (1985).

[33]C. Delalande, G. Bastard, J. Orgonasi, J. A. Brum, H. W. Liu, and M. Voos, Phys. Rev. Lett. **59**, 2690 (1989).

[34]C. Webber, C. Klingshirn, D. S. Chemla, D. A. B. Miller, J. E. Cunningham, and C. Ell, Phys. Rev. B **38**, 12 748 (1988).

[35]D. A. Kleinman, Phys. Rev. B **32**, 3766 (1985).

[36]E. O. Kane, in *Tunneling Phenomena in Solids,* edited by E. Burstein and S. Lundquist (Plenum, New York, 1969), p. 1.

[37]D. F. Nelson, R. C. Miller, and D. A. Kleinman, Phys. Rev. B **35**, 7770 (1987).

[38]W. Potz, J. Appl. Phys. **66**, 2458 (1989).

[39]P. M. Solomon, S. L. Wright, and C. Lanza, Superlatt. Microstruct. **2**, 521 (1986).

[40]C. S. Kyono, V. P. Kesan, D. P. Neikirk, C. M. Maziar, and B. G. Streetman, Appl. Phys. Lett. **54**, 549 (1989).

[41]Values for the Γ-X conduction-band offset in the literature range from 0.13 [E. E. Mendez, W. I. Wang, E. Calleja, and C. E. T. Goncalves da Silva, Appl. Phys. Lett. **50**, 1263 (1987)] to 0.20 eV [J. Batey and S. L. Wright, J. Appl. Phys. **59**, 200 (1986)]. We use the latter, more commonly favored value and neglect quantum confinement effects in the X valleys.

[42]E. E. Mendez, E. Calleja, and W. I. Wang, Appl. Phys. Lett. **53**, 977 (1988).

[43]B. Rheinlander, H. Neumann, P. Fischer, and G. Kuhn, Phys. Status Solidi B **49**, K167 (1972).

[44]A. C. Marsh, Semicond. Sci. Technol. **1**, 320 (1986).

[45]A. R. Bonnefoi, R. T. Collins, T. C. McGill, R. D. Burnham, and F. A. Ponce, Appl. Phys. Lett. **46**, 285 (1985).

[46]A. R. Bonnefoi, T. C. McGill, and R. D. Burnham, Phys. Rev. B **37**, 8754 (1988).

[47]P. J. Price, Surf. Sci. **196**, 394 (1988).